ACCOUNTS of chemical research

pubs.acs.org/accounts Article

Using Light and Electrons to Bend Carbon Dioxide: Developing and Understanding Catalysts for CO_2 Conversion to Fuels and Feedstocks

Published as part of the Accounts of Chemical Research special issue "CO2 Reductions via Photo and Electrochemical Processes".

Kailyn Y. Cohen, Rebecca Evans, Stephanie Dulovic, and Andrew B. Bocarsly*

Cite This: *Acc. Chem. Res.* 2022, 55, 944–954 Read Online

ACCESS | Metrics & More | Article Recommendations

CONSPECTUS: Our global society generates an unwieldy amount of CO_2 per unit time. Therefore, the capture of this greenhouse gas must involve a diverse set of strategies. One solution to this problem is the conversion of CO_2 into a more useful chemical species. Again, a multiplicity of syntheses and products will be necessary. No matter how elegant the chemistry is, commercial markets often have little use for a small set of compounds made in tremendous yield. Following this reasoning, the Bocarsly Research Group seeks to develop new electrochemical and photochemical processes that may be of utility in the conversion of CO_2 to organic compounds. We focus on investigating proton-coupled charge transfer mechanisms that produce both C1 and carbon−carbon bonded products (C2+).

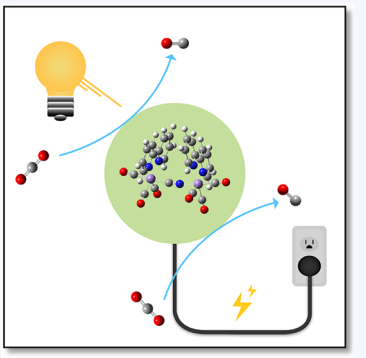

In early work, we considered the reduction of CO_2 to formate at electrocatalytic indium and tin electrodes. These studies demonstrated the key role of surface oxides in catalyzing the reduction of CO_2. This work generated efficient systems for the formation of formate and paved the way to studies using non-copper, intermetallic electrocatalysts for the generation of C2+ species. Most notable is the efficient formation of oxalate at an oxidized Cr_3Ga electrode. Oxalate has recently been suggested as a potential nonfossil, alternate organic feedstock.

Separately, we have focused on the electrocatalytic effects of pyridine on the reduction of CO_2 in aqueous electrolyte. These studies demonstrated that electrodes that normally yield a low hydrogen overpotential (Pd and Pt) show suppressed H_2 evolution and strongly enhanced activity for CO_2 reduction in the presence of pyridinium. Methanol was observed to form in high Faradaic yield at low overpotential using this system. The 6-electron, 6-proton reduction of CO_2 in the presence of pyridinium was intriguing, and significant effort was placed on understanding the mechanism of this reaction both on metal electrodes and on semiconducting photocathodes. P−GaP electrodes were found to provide exceptional behavior for the formation of methanol using only light as the energy source.

The pyridinium studies highlighted the role of protons in the overall reduction of CO_2, stimulating our interest in the chemistry of $MnBr(bpy)(CO)_3$ and related compounds. This complex was reported to electrochemically reduce CO_2 to CO. We saw these reports as an opportunity to study the detailed nature of the proton-coupled electron transfer (PCET) mechanism associated with CO_2 reduction. Our investigation of this system revealed the role of hydrogen-bonding in CO_2 reduction and pointed the way for the construction of a photochemical process for CO generation using a $[(bpy)(CO)_3Mn(CN)Mn(bpy)(CO)_3]^+$ photocatalyst.

Based on our studies to date, it appears likely that heterogeneous systems can be assembled to convert CO_2 into products that are "beyond C2 products." This may open up new practical chemistry in the area of fossil-based replacements for both synthesis and fuels. Systems with pragmatic efficiencies are close to reality. Electrochemical reactors using heterogeneous electrocatalysts show the stability and product selectivity needed to generate industrial opportunities. Continued growth of mechanistic understanding is expected to facilitate the chemical design of cogent systems for the taming of CO_2.

KEY REFERENCES

- Agarwal, J.; Shaw, T. W.; Schaefer, H. F.; Bocarsly, A. B. Design of a Catalytic Active Site for Electrochemical CO_2 Reduction with Mn(I)-Tricarbonyl Species. *Inorg. Chem.* **2015**, *54*, 5285−5294.[1] *This work seeks to understand the role of protons in the reduction of CO_2 to*

Received: October 15, 2021
Published: March 15, 2022

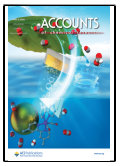

CO using a $MnBr(bpy)(CO)_3$ related homogeneous electrocatalyst. Hydrogen bonding between a manganese bound CO_2 and a pendent phenol (in the 6-position of the bipyridine ring) was found to dramatically enhance the catalytic process.

- Kuo, H.-Y.; Lee, T. S.; Chu, A. T.; Tignor, S. E.; Scholes, G. D.; Bocarsly, A. B. A cyanide-bridged di-manganese carbonyl complex that photochemically reduces CO_2 to CO. *Dalton Transactions* **2019**, *48*, 1226−1236.[2] *Although $MnBr(bpy)(CO)_3Br$ is easily decomposed in solution by exposure to visible light, it can be photostabilized by preparing the cyanide-bridged dimer, $[(bpy)(CO)_3Mn(CN)Mn(CO)_3(bpy)]^+$. This complex is found to be effective as both an electrocatalyst and a visible light photocatalyst for the reduction of CO_2 to CO.*
- Seshadri, G.; Lin, C.; Bocarsly, A. B. A new homogeneous electrocatalyst for the reduction of carbon dioxide to methanol at low overpotential. *J. Electroanal. Chem.* **1994**, *372*, 145−150.[3] *This is the first report that aqueous pyridine/pyridinium provides an electrocatalytic environment for the reduction of CO_2 to methanol. In this work, a hydrogen saturated palladium was found to produce high Faradaic efficiencies for methanol formation at low overpotential.*
- Barton, E. E.; Rampulla, D. M.; Bocarsly, A. B. Selective Solar-Driven Reduction of CO_2 to Methanol Using a Catalyzed p-GaP Based Photoelectrochemical Cell. *J. Am. Chem. Soc.* **2008**, *130*, 6342−6344.[4] *This work demonstrates the synthesis of methanol from CO_2 at an illuminated p-GaP cathode in the presence of aqueous pyridine/pyridinium. High Faradaic yield was observed at an underpotential, demonstrating that optical energy was efficiently powering the reaction.*

1. INTRODUCTION

According to the *New York Times* (July 7, 2021) based on data collected by The Scripps Institute and the National Oceanic and Atmospheric Administration (NOAA) separately, "Since [May 2014], emissions [of CO_2] have continued to soar. The latest full-year average, for 2019, was 409.8 parts per million, about 46 percent higher than the preindustrial average of 280. These findings continue to cast grave concerns by the geophysical community on the impacts of climate change."[5]

Out of these concerns, two research themes have developed, which are coalesced under the mantle of "Carbon Capture, Utilization, and Storage" (CCUS). Utilization specifically refers to the chemical conversion of carbon dioxide to value-added organic products. One of the research themes specifically focuses on the climate change crisis and the need to remove massive amounts of CO_2 from the atmosphere. Under this imperative, it is best to form a product that will remain "locked up" for a geologic time period. The second theme sees carbon dioxide as a valuable chemical feedstock that might replace fossil-based resources, both as a source of organic precursors and as a fuel. In this case, CO_2 need not be sequestered, but a chemistry of oxidized carbon (i.e., CO_2) must be developed that rivals today's chemistry of reduced carbon (i.e., fossil resources). Taken together, these two themes generate a synthetic carbon cycle that can supplement the natural carbon cycle that is overburdened by our current use of fossil fuels. Both branches of this cycle are endergonic, and thus, the cycle only works if it can be powered efficiently and by a non-fossil-fuel source of energy. To help meet this need, the Bocarsly Research Group is interested in the development of electrochemical approaches that efficiently and selectively generate desirable products from CO_2, using processes that can be driven by alternate energy resources. We are achieving this result by developing an understanding of the electrocatalytic reduction of CO_2 using both metal and semiconductor electrodes. In the case of metal electrodes, we focus on the mechanism and catalytic efficiency of CO_2 reduction at interfaces that can selectively carry out the desired multiple proton-coupled electron transfers (PCETs) under conditions where proton reduction to form H_2 competes with CO_2 reduction. Various formal reduction potentials for CO_2 reduction are found in Table 1. It should be noted that the similarity in the redox potential for the various products suggests that one cannot select between products formed by exerting potential control. The one exception to this statement being the one-electron reduction of CO_2 to CO_2^-. It should also be noted that introducing protons into the chemical reaction (PCET) dramatically lowers the energy of the reaction as measured by the redox potential. In passing, we note that this energy difference suggests that when protons are available, the carbon dioxide radical anion will not be involved in the reaction pathway. On the other hand, the redox potential for proton reduction to H_2 (0.00 V vs SHE) is similar to the PCET reduction potentials for CO_2. This indicates that proton-coupled reduction of CO_2 will always need to kinetically compete with the reduction of protons to water.

Table 1. Standard Redox Potentials for the Carbon Dioxide Half Reactions

reaction	E°_R, V vs SHE @ pH = 0
$CO_2(g) + e^- \rightarrow CO_2^{\bullet -}(aq)$	−1.90
$2CO_2(g) + 2e^- \rightarrow (CO_2)_2^{2-}(aq)$	−0.64
$2CO_2(g) + H^+(aq) + 2e^- \rightarrow H(CO_2)_2^-(aq)$	−0.52
$2CO_2(g) + 2H^+(aq) + 2e^- \rightarrow H_2(CO_2)_2(aq)$	−0.48
$CO_2(g) + H^+(aq) + 2e^- \rightarrow HCOO^-(aq)$	−0.19
$CO_2(g) + 2H^+(aq) + 2e^- \rightarrow CO(g) + H_2O(aq)$	−0.10
$CO_2(g) + 4H^+(aq) + 4e^- \rightarrow H_2CO(aq) + H_2O$	−0.07
$2H^+(aq) + 2e^- \rightarrow H_2(g)$	0.00
$CO_2(g) + 6H^+(aq) + 6e^- \rightarrow CH_3OH(aq) + H_2O$	0.04
$CO_2(g) + 8H^+(aq) + 8e^- \rightarrow CH_4(g) + 2H_2O$	0.17

In all cases, the processes of interest are thermodynamically uphill and therefore must be driven by an alternate electricity resource such as wind or solar-derived electricity. This can be accomplished by coupling an alternate energy resource to a standard electrochemical cell. Alternately, one can utilize a cathode composed of a p-type semiconductor to generate photoelectrochemical cells where the reduction of CO_2 is driven by the direct absorption of light by the photocathode. In these latter systems, the synthesis of an active and stable interface presents the project goal.

Both approaches hinge on the ability to design and optimize the electrocatalytic nature of the electrode−electrolyte interface. To this end, one needs to consider both heterogeneous PCET occurring at a catalytically active electrode surface and homogeneous electrocatalysis in which a solution species mediates the flow of electrons and protons between the electrode and the CO_2 catholyte. While the practicalities of system long-term stability and high current densities favor the implementation of a heterogeneous electrocatalytic interface,

https://doi.org/10.1021/acs.accounts.1c00643
Acc. Chem. Res. 2022, 55, 944−954

mechanistic understanding of electrocatalytic processes is much more accessible using molecular systems. Additionally, molecular systems provide the opportunity to develop purely photochemical approaches to CO_2 reduction. Therefore, we are also interested in dissolved transition metal complexes that photochemically transform CO_2 to CO.

It is well appreciated that one of the challenges in converting CO_2 into organic products is the exceptionally high reaction barrier associated with the first electron transfer. In significant part, that barrier is associated with the fact that the linear CO_2 molecule must rehybridize to generate the anion. That is, the sp hybrid associated with bonding in carbon dioxide must be decreased in s-character to form the anion. As shown in Figure 1, the direct result of this rehybridization is a decrease in the

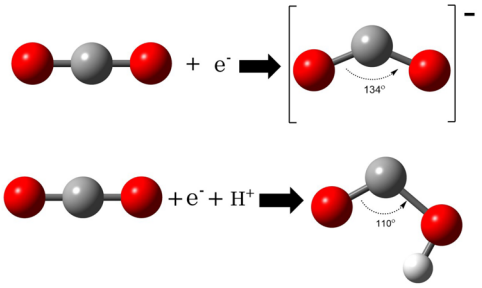

Figure 1. Bending CO_2. One electron reduction of CO_2 rehybridizes the frontier orbitals producing the anionic bent structure shown in the upper right of this figure. A lower degree of rehybridization is required forming an sp^3 hybrid, if the electron transfer is accompanied by a proton transfer.

CO_2 bond angle as $[CO_2]^{\bullet-}$ is formed. Thus, the kinetic activation of CO_2 can be thought of as the process of bending.

Facilitating this geometric change is a matter of developing a reaction environment that enhances the rehybridization using a barrier lowering electrocatalyst. DFT calculations indicate that the reaction in Figure 1 requires ∼108 kJ/mol and generates a bond angle of 134° indicating a hybrid state that is approximately $sp^{3/2}$. Adding a proton to this system (PCET) to generate OCOH (bottom of Figure 1) decreases the O−C−O bond angle to 110°, generating approximately sp^3 hybridization. This lowers the energy needed to carry out the electron transfer. Similar kinetic improvement can be obtained by coordinating the CO_2 reactant to a metal surface or transition metal ion, thereby encouraging the necessary rehybridization. This simple analysis, of course, ignores the other major reaction challenge in the carbon dioxide system: how can carbon−carbon bonds be formed with a minimal expenditure of energy? This challenge is equal to the bond angle challenge and is a current area of interest in the Bocarsly Research Group.

2. HETEROGENEOUS CARBON DIOXIDE REDUCTION

Within the realm of heterogeneous electrocatalysis, our group has explored copper-free metallic surfaces that are catalytically reactive, generating C1 products such as formate and methanol from CO_2, as well as more intriguing (and complex) metal-based interfaces that can promote the formation of C2+ products. These C2+ products include oxalate, acetic acid, ethanol, propanol, and acetone. Attention has been placed on heavy post-transition metals (In, Sn, Bi, Pb) as catalysts for CO_2 to formate (i.e., pure C1 chemistry), as these metals have been previously identified to do selective 2-electron reductions.[6] Our investigation started with In, where we hypothesized that the reaction of interest occurred at a clean metal surface. However, it was revealed that the presence of a surface hydroxide, in the form of $In(OH)_3$, was critical to CO_2 reduction to formate.[7] Similarly, the surface species on a tin electrode, $Sn(II)(OH)_2$, was found to be responsible for the observed CO_2 reduction chemistry.[8] In both cases, the generation of formate was made possible by the insertion of CO_2 into the surface species to form a surface bicarbonate intermediate. Further examination of the post-transition metals observed mechanisms for the Pb and Bi electrodes that differed from the In and Sn electrodes. While In and Sn can be considered oxide-active materials, Pb can be regarded as an oxide-buffered material, where the oxide does not participate directly in CO_2 reduction to form a surface bicarbonate. Instead, these oxide-buffered materials provide a buffering effect at the electrode/electrolyte interface that supplies protons required for the electroreduction. Bismuth differs from the previous two materials as it is oxide-independent, meaning the oxide species does not impact the desired electrochemistry.[14]

Copper and other metals such as Ru and Mo were reported in the late 1970s and early 1980s to reduce CO_2 to C1 species.[6,15,16] However, only Cu could accomplish higher-order electrochemical reduction of CO_2 to multicarbon species. This remained true until recently, when the Lewis group at California Institute of Technology showed that various Ni_xGa_y intermetallics were capable of CO_2 reduction to ethane and ethylene, reaching Faradaic efficiencies (ξ) of approximately 1.5% and 0.5%, respectively.[9] Faradaic efficiencies are calculated using eq 1.

$$\xi = \frac{Q_{\text{product}}}{Q_{\text{total}}} \tag{1}$$

Table 2. Faradaic Efficiencies and Electrode Potentials of Various Bimetallic Systems for CO_2 Reduction

bimetallic system	products (ξ)	E (V vs SHE)	ref
Ni_5Ga_3/HOPG	methane (∼2%), ethane (∼1.7%), ethylene (∼0.4%)	−0.48	9
Ni_3Ga/GC	CO (11.2%), formate (0.23%), methanol (0.06%)	−1.18	10
Ni_3Ga/RVC	CO (26%), formate (1.0%), methanol (0.10%)	−1.18	10
Ni_3Ga/HOPG	ethane (0.10%)	−1.18	10
Ni_3Al/GC	CO (33%), 1-propanol (1.9%), methanol (1.0%), formate (0.75%)	−1.18	11
Ni_3Al/RVC	CO (33%), 1-propanol (0.27%), methanol (0.22%), formate (0.18%)	−1.18	11
Ni_3Al/HOPG	CO (0.78%), 1-proponol (0.34%), methanol (0.20%), formate (0.15%)	−1.18	11
$CuInSe_2$/[Ni_3Al+TiO_2]	methanol (25%)	−0.60	12
$(Cr_2O_3)_3(Ga_2O_3)$/GC	oxalate (59%), CO (8.1%), formate (0.16%), methanol (0.15%)	−1.28	13

https://doi.org/10.1021/acs.accounts.1c00643
Acc. Chem. Res. 2022, 55, 944−954

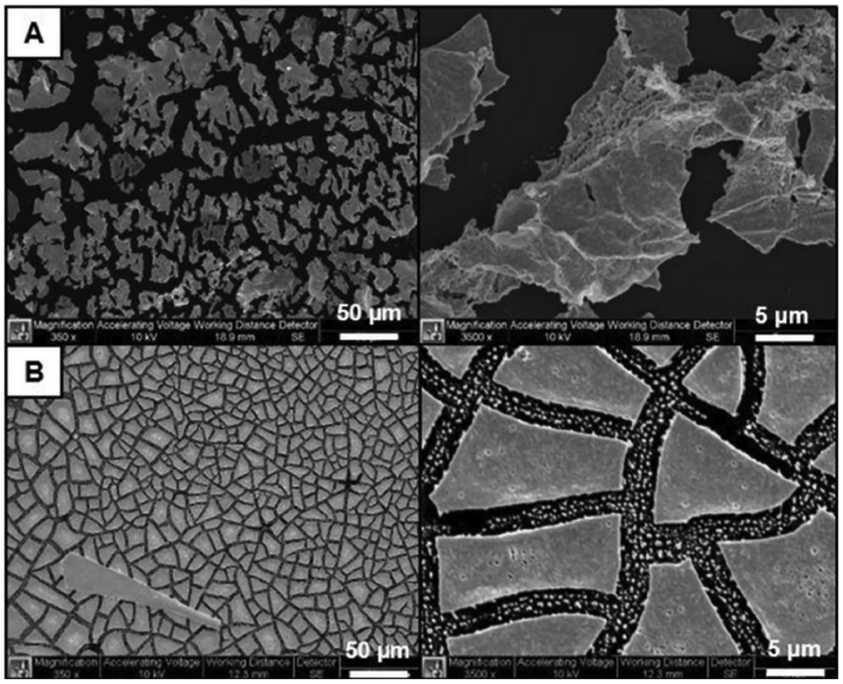

Figure 2. SEM images of Ni_3Ga thin films synthesized on (A) HOPG and (B) glassy carbon at low (left) and high (right) magnification. While HOPG-plated films are comprised of layered microparticles, glassy carbon variants consist of relatively uniform platelets distributed across the surface. Reproduced with permission from ref 10. Copyright 2018 IOPscience.

This report was significant because the onset potential for the observed products was found to be −0.48 V vs RHE, which was among the lowest observed for C2 products. This result inspired us to explore intermetallic systems involving a first-row transition metal coupled with a group 13 metal. Various reduction potentials and Faradaic efficiencies for CO_2 reduction using bimetallic systems are displayed in Table 2. We chose the very general M_3N stoichiometry and found that Ni_3Ga, Ni_3Al, and $(Cr_2O_3)(Ga_2O_3)$ systems were electrocatalytic for C2+ products. The products detected varied for the different mixed metal systems, with C2+ ξ values in the range of 0.1% to 2%. However, a highlight of the Cr/Ga system is the ability to generate oxalate in yields as high as 60%.[13] The observation of high Faradaic efficiency for oxalate formation in aqueous electrolyte is notable for two reasons. First, although oxalate has been previously electrosynthesized, it has required the use of a nonaqueous electrolyte and large overpotentials.[17] Using the Cr/Ga system, good Faradaic efficiency was achieved in aqueous electrolyte at −1.48 V vs Ag/AgCl. This represents a ∼700 mV overpotential, which is much less than previously observed. Second, oxalate is the only two electron system that generates a carbon−carbon bond from CO_2 and as such provides a gateway to C2+ organics. Recently, Gruter et al. pointed out that oxalate offers a broad spectrum of opportunities as a feedstock for a variety of organics.[18] Of primary interest is the conversion of oxalate to glycolic species, which have utility in a variety of pragmatic synthetic applications. Gruter has suggested that oxalate may be a considered a "drop in" alternative feedstock for a wide variety of petroleum-based products.[18]

In our investigation of the Cr/Ga systems, the presence of both oxides proved to be crucial in producing multicarbon products, and it is possible that the presence of surface metal oxide species may be necessary for the observed chemistry for the other intermetallic systems. In the study of Ni_3Ga thin films, we demonstrated that the products formed were exquisitely sensitive to the electrode material. Thus, for example, switching from a highly ordered pyrolytic graphite (HOPG) electrode to a glassy carbon electrode shut down C2 formation, even though both electrodes are nominally composed of a graphite phase. This result is ascribed to a catalyst deposition effect influenced by the solid support, in which the use of different supports led to altered surface morphologies and electrochemical behaviors.[10]

Specifically, Ni_3Ga on HOPG has a distinct rough surface in comparison to Ni_3Ga on glassy carbon, which has a flat and more uniform structure, shown in Figure 2. It is hypothesized that C−C coupling is possible because the high surface area of the Ni_3Ga promoted by the HOPG allows surface-bound intermediates to be in close proximity. Given this finding, it is not quite as surprising that different product yields are observed using a Ni_3Al catalyst distributed on glassy carbon versus a CIGS (copper, indium, gallium, selenium) based p-type photoelectrode.[10,12,13]

In contrast to the above approach, we have also explored the chemistry involved in the homogeneous electroreduction of CO_2. Presently, our main vehicle for doing this is complexes based on a $MnXbpy(CO)_3$ motif, which is highly selective for the conversion of CO_2 to CO. However, we have also explored the reduction of CO_2 to C1 and C2+ products using protonated aromatic amines such as pyridinium and imidazole.[19] While acting in solution, these compounds appear to have a significant inner sphere role under catalytic conditions that brings in some aspects of heterogeneous catalysis. These compounds are excellent for the conversion of CO_2 to formate and methanol; however, we have also found that carbon−carbon coupling is possible with appropriate substitution of the aromatic amine catalyst.

https://doi.org/10.1021/acs.accounts.1c00643
Acc. Chem. Res. 2022, 55, 944−954

3. HOMOGENOUS CARBON DIOXIDE REDUCTION USING PYRIDINE AND AROMATIC AMINES

We first observed the ability of pyridinium to electrocatalyze the reduction of CO_2 in 1994 through happenstance and hypothesis testing. Initial tests were conducted using a hydrogenated Pd electrode (β-PdH phase) with 10 mM added pyridine in aqueous electrolyte. The solution was adjusted to pH 5.4, an approximate 1:1 mixture of pyridine and pyridinium (pK_a = 5.25), which conveniently buffered the system and interestingly generated hydrogen bonded pyridine−pyridinium pairs.[20] The aqueous Raman spectrum of $[py{-}H{-}py]^+$ is shown in Figure 3.

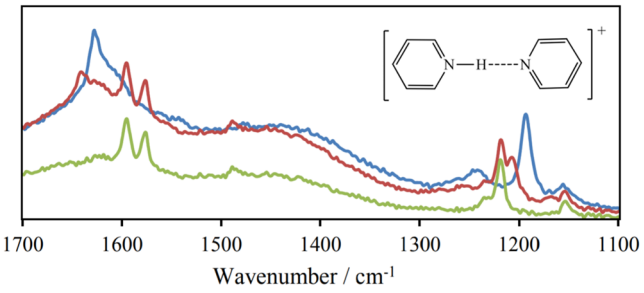

Figure 3. Raman spectra of pyridinium in water (blue) and an equilibrium mixture of $[py{-}H{-}py]^+$ and $[pyH]^+$ in water (red). Subtraction of the pure pyridinium spectrum from the mixture spectrum yields the aqueous $[py{-}H{-}py]^+$ spectrum (green). Adapted with permission from ref 20. Copyright 2014 Taiwan Association for Aerosol Research.

Cyclic voltammetric studies under either Ar or CO_2 suggested an electrocatalytic mechanism that involved a PCET cycle. Bulk electrolysis experiments with aqueous solutions containing both CO_2 and pyridine revealed the formation of formaldehyde and methanol. These products were authenticated using ^1H NMR, colorimetric indicators, mass spectroscopic and gas chromatographic data. Further ^{13}C experiments validated that these products were produced from CO_2 and not by degradation of the pyridine catalyst or any other carbon source. While many CO_2 reduction systems function at high overpotentials, one of the draws of these initial experiments was the low overpotential (200 mV) needed to reduce CO_2 to methanol at a Pd electrode.[3]

The pyridinium-assisted reduction of CO_2 on both Pd and Pt electrodes was exported to a light-driven p-GaP electrode system, which efficiently (Faradaic efficiencies ranged from 88% to 100%) formed methanol when illuminated at 365 nm.[4] At −0.5 V vs SCE, the highest quantum yield for the 6-electron reduction to form methanol was 44%, yielding a 10.9% optical energy conversion efficiency.[4] Other electrode systems and their Faradaic efficiencies for the conversion of carbon dioxide to methanol are shown in Table 3. Similar to the p-GaP electrode, experiments were conducted using a p-FeS_2 electrode to reduce CO_2. However, unlike p-GaP and Pd electrodes, the p-FeS_2 electrode was only capable of reducing CO_2 to formic acid and carbon monoxide. Both pyridine and imidazole were found to be effective electrocatalysts in this system.[19] Our work also indicated that other aromatic amines were able to enhance the reduction of CO_2, including 1-ethyl-3-methyl imidazolium, which was proposed to operate through an N-heterocyclic carbene ylide-like intermediate.

Table 3. Comparison of Electrode Potentials and Efficiencies for the Conversion of Carbon Dioxide to Methanol

electrode	E (V vs SHE)	Faradaic efficiency (%)	ref
p-GaP	−1.16	60	21
p-GaAs	−1.16	55	22
p-InP	−1.06	70	22
n-GaAs	−1.06	100	22
Cu	−0.86	40	23
Cu/Cd	−1.51	5	24
Cu/PdH	−1.36	5	25
Ru	−0.30	42	16
Ru/Cu	−0.56	40	26
RuO_2/TiO_2	−0.71	30	27
RuO_2/TiO_2	−0.56	60	28

In addition to the experimental work of our group,[3,4,20,29−33] the 6-electron reduction of CO_2 to methanol in the presence of pyridinium at a Pd electrode has been computationally explored by Batista,[33,34] Musgraves,[35−38] and Keith and Carter.[39−42] The mechanism of CO_2 photoelectrochemical reduction using p-GaP/pyridinium has also been extensively investigated by some of the same parties: Bocarsly,[4] Carter,[43−45] and Musgraves.[37] While there are still disagreements about a suitable mechanism most notably voiced by Savéant,[46] there is general agreement that the mechanism is surface confined, involving inner sphere and hydrogen atom transfer processes. The various mechanistic possibilities in this system have been previously reviewed by Lakkaraju, Bocarsly and co-workers.[47]

4. HOMOGENEOUS CARBON DIOXIDE REDUCTION INVOLVING MANGANESE COMPLEXES

Lehn et al. were the first to report that *fac*-ReCl(bpy)$(CO)_3$ was a photo- and electrocatalyst for the reduction of CO_2 to CO.[48] While this complex is able to act as both a homogeneous catalyst and photosensitizer, Lehn and co-workers found that photodecomposition occurs under near-UV irradiation, which is needed to perform the reaction.[49]

It was not until 2011 that the first analogous manganese polypyridyl electrocatalyst, MnBr(bpy)$(CO)_3$, was reported by Deronzier et al.[50] This was nearly 50 years after the synthesis of *fac*-MnI(bpy)$(CO)_3$ was reported in 1959 by Abel and Wilkinson.[51] One of the greatest challenges associated with utilizing Mn polypyridyl complexes is their extreme photosensitivity in solution, which leads to decomposition upon exposure to room light via loss of CO ligands. This prevents them from acting as photochemical reagents and poses an additional challenge in studying them electrochemically.

In order to explore this chemistry further, a complex was needed that did not undergo rapid photochemical degradation under room light. However, given that MnBr(bpy)$(CO)_3$ was already a known electrocatalyst, our research group was initially interested in the electrocatalytic mechanism and catalytic efficiency. In an effort to circumvent this problem, we presented the synthesis and characterization of the first catalytic manganese N-heterocyclic carbene complexes for the electrocatalytic reduction of CO_2 to CO in 2014.[52] Based on the manganese(I) complexes following the form *fac*-MnBr(N−N)$(CO)_3$, where N−N is a bpy ligand, a single pyridine ring in bpy was replaced with one N-heterocyclic carbene (NHC) moiety to change the metal coordination environment. The

https://doi.org/10.1021/acs.accounts.1c00643
Acc. Chem. Res. 2022, 55, 944−954

advantage of such an approach allows for the incorporation of NHC ligands that are 4-, 5-, or 6-membered.

Under an atmosphere of CO_2, both manganese NHC-pyridine species showed a current enhancement that fell only slightly below that of the parent complex, $MnBr(bpy)(CO)_3$ when in wet (5% v/v H_2O) MeCN with 0.1 M tetrabutylammonium perchlorate (TBAP) as the supporting electrolyte. We also reported that the first- and second-electron reductions occurred at approximately the same potential for both NHC-pyridine containing complexes when compared to the parent compound, which showed a difference between the two sequential one-electron reductions of several hundred millivolts. Consistent with an electron transfer−chemical reaction−electron transfer (ECE) mechanism, the first reduction wave of the NHC-pyridine complex corresponded to the formation of a doubly reduced anionic species, followed by the loss of the bromide anion. This allows for the coordination and subsequent two-electron reduction of CO_2 to CO. The second, smaller reduction peak was reported to correspond to the reduction of a small quantity of a Mn−Mn dimer species, $[\{Mn(NHC\text{-}pyridine)(CO)_3\}_2]$.

As previously stated, one of the major problems with working with these Mn complexes was their rapid photochemical degradation under room light. To see whether the photostability of these complexes could be improved, we replaced the Br^- axial ligand of $MnBr(N{-}N)(CO)_3$ with either CN^- or NCS^- to explore the effect of the axial ligand on photodecomposition.[53] By substituting CN^- for Br^-, we were able to improve the photostability of the complex significantly (5×) under 420 nm illumination due to resulting blue-shifted MLCT band. For $MnBr(Et\text{-}Im\text{-}Py)(CO)_3$ and $MnNCS(Et\text{-}Im\text{-}Py)(CO)_3$, the initial yellow complexes in DMSO quickly turned red-brown when exposed to room light, whereas the two complexes with CN ligands in the axial position, $MnCN(Et\text{-}Im\text{-}Py)(CO)_3$ and $MnCN(Et\text{-}BIm\text{-}Py)(CO)_3$ remained their initial yellow color even after many days of exposure to room light. This was attributed to the strong-field nature of the cyanide ligand relative to thiocyanate and bromide.

While the manganese polypyridyl complexes have similarities to their rhenium counterparts, one notable difference is that manganese complexes require the addition of weak Brønsted acids in order to reduce CO_2 to CO.[53,54] The effect of a Brønsted acid upon the system is thought to be 2-fold: (1) the acid will stabilize the O atom of CO_2 through hydrogen bonding and (2) it will facilitate C−O bond cleavage of CO_2 needed to produce CO.[55] As shown in Figure 4, to compare the effects of intermolecular and intramolecular H-bonding, we were able to incorporate an intramolecular H-bond in the second coordination sphere by adding a phenol in the 6-position of the bipyridine ring.[56] The resulting ligand, 6-(2-hydroxyphenyl)-2,2′-bipyridine (HOPh-bpy), would then be able to coordinate to the O of CO_2.

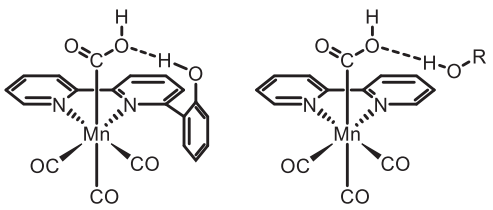

Figure 4. Schematics of the manganese complexes comparing intramolecular hydrogen bonding (left) vs adding a Brønsted acid (right). Adapted with permission from ref 56. Copyright 2015 American Chemical Society.

Under an atmosphere of CO_2, $MnBr(HOPh\text{-}bpy)(CO)_3$ was reported to display an 11-fold current enhancement from 0.58 mA/cm^2 to 6.3 mA/cm^2 at the potential of the second reduction wave. This current enhancement was 7 times greater than the current enhancement seen for $MnBr(bpy)(CO)_3$ at approximately the same overpotential. To investigate whether the improved CO_2 reduction was due to the presence of a phenolic proton in the second coordination sphere, the 6-position of bpy was replaced with anisole to form $MnBr(MeOPh\text{-}bpy)(CO)_3$. This complex only displayed a 2.1× current enhancement under CO_2 atmosphere, indicating that the current increase was in fact due to the phenolic proton. When only 1 mM $MnBr(bpy)(CO)_3$ was evaluated with wet (5% v/v water) MeCN with and without 10 mM phenol, the catalytic rate was observed to decrease with the addition of phenol. This confirmed that the addition of phenol alone could not be responsible for the current enhancement observed for $MnBr(HOPh\text{-}bpy)(CO)_3$. Using theory, we suggested that the source of this increased activity came from a lower entropic barrier to an intramolecular mechanism for proton-assisted dehydration of the $Mn(6\text{-}(2\text{-}hydroxyphenyl)\text{-}bpy)(CO)_3COOH$ intermediate.[1]

Later, in 2019, we presented a mechanistic study that explored the viability of the proposed pendent H-bond donors.[57] While the previous study attached H-bond donors in the 6-position of the bipyridine ring, this study synthesized $MnBr(HOPh\text{-}bpy)(CO)_3$ analogues, in which HOPh was placed in the 4- and 5-positions as well. This was in addition to comparing the electrocatalytic activity of the same complexes using MeOPh instead, which does not have H-bonding ability. We observed that significant current enhancement for CO_2 reduction was only seen when the H-bond donor was in the 6-position on the bipyridine ring, as this would be the closest position to the ligated Mn center. The X-ray structures also showed that the 4- and 5-substituted complexes had increased torsion angles between the phenol and bipyridine ring relative to the 6-substitued complex as a result of increased steric interference between the phenol and Mn center.

More recently, we synthesized a variety of *fac*-$MnBr(N{-}N)(CO)_3$ complexes, shown in Figure 5, where the N−N ligand was 1,10-phenanthroline, bipyrizine, or bipyridine.[58] This was done in order to understand the effects on the bipyridine π^* energy level and the electrocatalytic conversion of CO_2 to CO. UV−vis, cyclic voltammetry, and density functional theory calculations were employed showing that adding electron-withdrawing substituents to the 4,4′-position of the bipyridine ligand red-shifted the MLCT band, leading to poorer CO_2 conversion to CO. The LUMO energy levels, which correlated to the bpy π^* energy level, were calculated to be more negative as electron withdrawing groups were incorporated on the bpy. This led to smaller MLCT energy and a positive shifted first peak potential. The resulting decrease in CO_2 conversion was attributed to slower axial Br^- loss, as the internal conversion from the bpy π^* orbital to the metal d−σ^* scaffold of orbitals became more difficult with a smaller MLCT energy gap. Second, the HOMO of the doubly reduced species was less electron dense with electron-deficient complexes, making it more difficult to bind to CO_2.

One of the proposed intermediates of the monomeric $MnBr(bpy)(CO)_3$ electrocatalytic cycle is believed to be the

https://doi.org/10.1021/acs.accounts.1c00643
Acc. Chem. Res. 2022, 55, 944−954

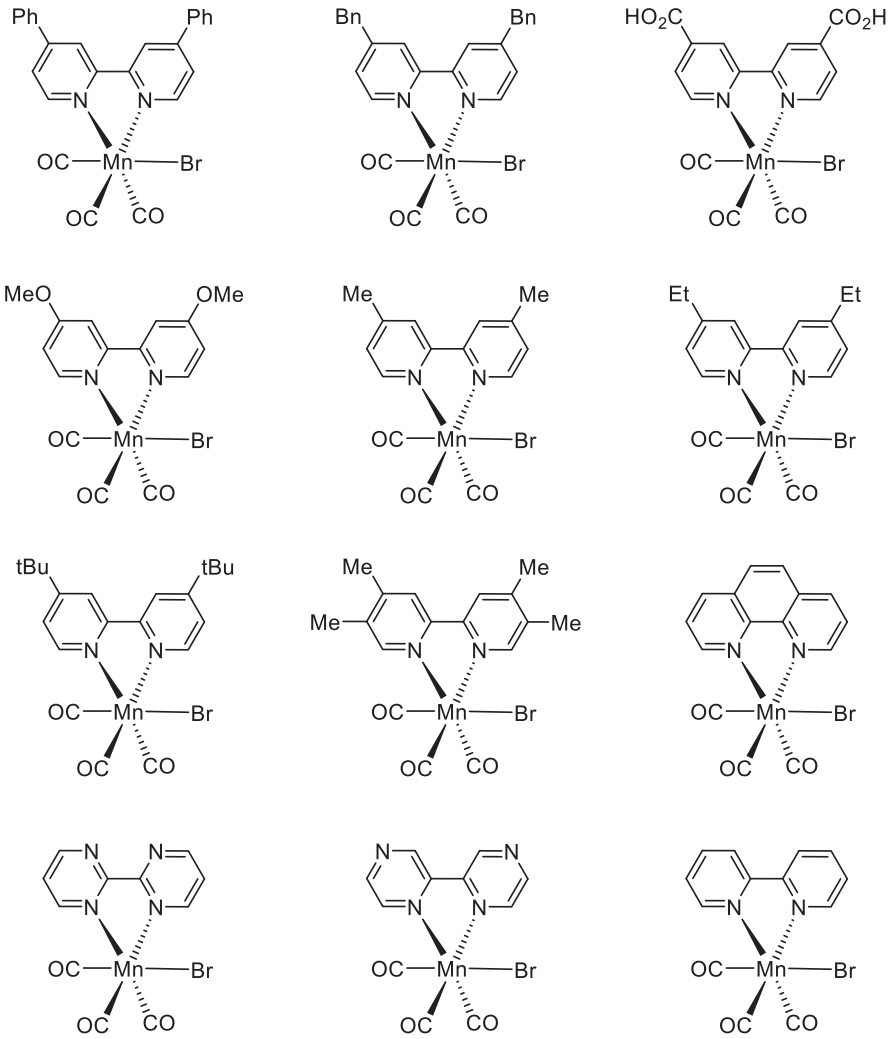

Figure 5. Scope of manganese complexes synthesized. Adapted with permission from ref 58. Copyright 2019 American Chemical Society.

tricarbonyl complex, $[Mn(bpy)(CO)_3]^-$. During this cycle, shown in Figure 6, the cationic tetracarbonyl complex is thought to form in solution after reaction with CO_2 and two protons. We successfully synthesized the tetracarbonyl intermediate and characterized it via IR and UV−vis spectroscopy.[59] It was found through in situ UV−vis under Ar, that at the second reduction potential (−1.88 V vs Fc/Fc^+) both $[Mn(bpy)(CO)_3]^-$ and the Mn−Mn bonded dimer formed. It was also reported using IR spectroscopy before and after electrolysis at the first reduction potential (−1.48 V vs Fc/Fc^+) that both $[Mn(bpy)(CO)_3]^-$ and the Mn−Mn bonded dimer formed. Radiolabeled $^{13}CO_2$ was employed, and via gaseous IR spectroscopy it was shown that $^{13}CO_2$ could be electrocatalytically converted to ^{13}CO. Though the axial ligand in the Mn parent complex, which has been identified to dissociate first, is typically a halide, such as Br^-, we found through IR analysis that axial CO dissociation will occur after the complex has been singly reduced. In essence, the axial ligand need not necessarily be a halide for CO_2 electroreduction to occur.

As a result of the extreme photosensitivity of Mn complexes, various groups such as ours have attempted to modify the $[MnX(N-N)(CO)_3]$ scaffold (where N−N is a polypyridyl ligand) in an effort to improve its photostability.[60−65] Building upon our group's previous work of shifting the MLCT band into the UV-region by substituting the axial Br^- ligand with a CN^- ligand, a novel CN-bridged dimer was synthesized to enhance the photostability of these Mn complexes.[2]

By substituting the Br^- axial ligand of the monomer species with the strong π-acceptor, CN^-, the MLCT band was shifted from 417 to 375 nm, which led to the development of a novel, cationic cyanide-bridged dimanganese species, $\{[Mn(bpy)(CO)_3]_2(\mu\text{-}CN)\}ClO_4$. This species, abbreviated Mn_2CN^+, is represented in Figure 7 and features a MLCT at 364 nm. We demonstrated that Mn_2CN^+ was both electrocatalytically and photochemically active for CO_2 reduction to CO without the introduction of an added photosensitizer.

In a 4 h bulk electrolysis with the potential held near the second reduction peak at −1.90 V vs Fc/Fc^+, $MnBr(HOPh\text{-}bpy)(CO)_3$, Mn_2CN^+, displayed a maximum ξ of 90%, compared to the ξ of the parent complex $MnBr(bpy)(CO)_3Br$, which was at 75%. While the use of $MnBr(bpy)(CO)_3$ and $MnCN(bpy)(CO)_3$ to photochemically reduce CO_2 to CO is implausible without an added photosensitizer given their rapid photodegradation, the Mn_2CN^+ complex was able to photochemically reduce CO_2 with either 5% v/v water or 1 M phenol as the proton source in CO_2-saturated MeCN. Using radiolabeled $^{13}CO_2$, we were able to show via FT-IR spectroscopy that the CO produced arose from CO_2 reduction.

https://doi.org/10.1021/acs.accounts.1c00643
Acc. Chem. Res. 2022, 55, 944−954

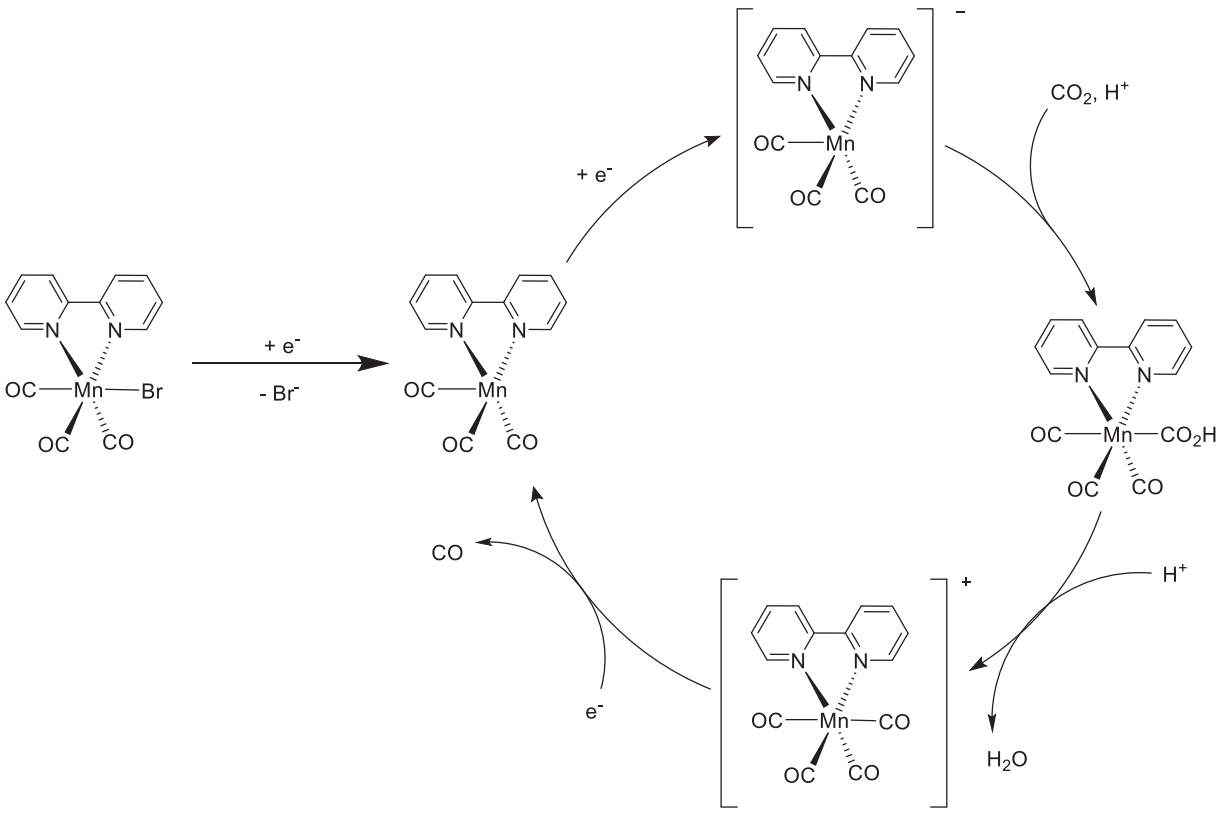

Figure 6. Electrocatalytic cycle for $MnBr(bpy)(CO)_3$ reducing CO_2 to CO. Adapted with permission from ref 58. Copyright 2019 American Chemical Society.

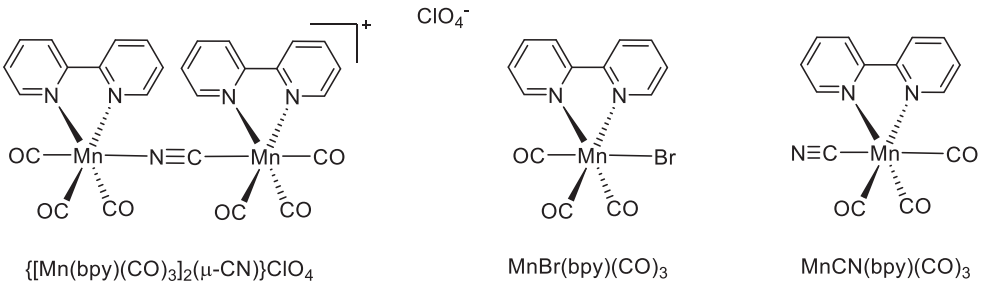

Figure 7. Representations of the cyanide bridged dimanganese species and its two monomeric precursors. Reproduced with permission from ref 2. Copyright 2019 The Royal Society of Chemistry.

The photophysical properties of Mn_2CN^+ were studied via UV−vis and IR under irradiation at 365 nm. The UV−vis displayed a shoulder that rose around 520 nm and a clear isosbestic point at 420 nm after irradiation, indicating a one-to-one conversion of Mn_2CN^+ into a photoproduct. IR studies revealed that upon irradiation, the carbonyl peak trans to the C of the bridging cyanide ligand selectively disappeared. It was thought that the photoproduct was a solvato species, where the coordinating MeCN solvent replaced the CO_{axial} on the C-end of the complex. We also showed that using 2-MeTHF, a weakly coordinating solvent, did not result in the formation of an isosbestic point in the UV−vis.

Additional FT-IR studies with continuous photolysis revealed that peaks evolved at 1870 and 2120 cm^{-1}, corresponding to a carbonyl stretching mode and a shifted bridged-CN mode postirradiation.[66] DFT calculations indicated that these features were unique to the solvated species, s-Mn_2CN^+, in which the axial position trans to the C-end of the bridging cyanide ligand was coordinated by MeCN, rather than on the N-end of the molecule. Transient absorption spectroscopy was also employed, showing that the excited state lifetime of Mn_2CN^+ was 7 ns and was stabilized by coordinating MeCN solvent.

5. FUTURE DIRECTIONS

A variety of scientific challenges remain in the understanding of CO_2 chemistry at a level that could lead to practical systems for the efficient utilization of this compound as a fossil fuel substitute. All of the fuel and feedstock transformations of interest to our group are thermodynamically uphill processes. Thus, energy requirements must be meticulously considered, with the differences between activational free energies and free energies of reaction carefully segregated and regulated. Control over the hydrogen-bonding environment, interfacial proton gradients, and coupling of multielectron and electron−proton processes all provide access to the lowest energy reaction channels.

https://doi.org/10.1021/acs.accounts.1c00643
Acc. Chem. Res. 2022, 55, 944−954

The largest and perhaps most important challenge in carbon dioxide electrochemistry is understanding and controlling carbon−carbon bond formation. To date, very few systems are known that are able to carry out the transformation of CO_2 to C2+ products. It is a mastery of these reactions that will allow CO_2 to truly become an alternate chemical platform to fossil-based resources.

Currently, we only have a partial understanding of the multiple charge carrier processes and even less of an understanding of how to control such processes. Thus, the rational design of both molecular and electrode interfacial electrocatalysts remains out of immediate reach. Yet, our understanding of such interactions is close to the point of application. Therefore, it is reasonable to believe that in the near future, the regulated activation of carbon dioxide will be a matter of applying rules that regulate multi-PCET processes. At the current time, we are mainly observers of chance systems that generate hydrocarbons from CO_2. A detailed mechanistic understanding of these reactions is essential to the further development, control, and application of CO_2 as a feedstock chemical, while providing a non-fossil-fuel-based entry point to the organic chemistry on which our society depends.

AUTHOR INFORMATION

Corresponding Author

Andrew B. Bocarsly − *Frick Laboratory, Department of Chemistry, Princeton University, Princeton, New Jersey 08544, United States;* orcid.org/0000-0003-3718-0933; Email: bocarsly@princeton.edu

Authors

Kailyn Y. Cohen − *Frick Laboratory, Department of Chemistry, Princeton University, Princeton, New Jersey 08544, United States;* orcid.org/0000-0002-6912-5747

Rebecca Evans − *Frick Laboratory, Department of Chemistry, Princeton University, Princeton, New Jersey 08544, United States*

Stephanie Dulovic − *Frick Laboratory, Department of Chemistry, Princeton University, Princeton, New Jersey 08544, United States*

Complete contact information is available at: https://pubs.acs.org/10.1021/acs.accounts.1c00643

Author Contributions

The manuscript was written through contributions of all authors. All authors have given approval to the final version of the manuscript.

Notes

The authors declare no competing financial interest.

Biographies

Kailyn Y. Cohen graduated from Ursinus College in 2020 with a B.S. in Chemistry and earned her M.A. degree from Princeton University in 2022. Her undergraduate research focused on the electrochemistry of bimetallic proteins as well as carbon dioxide photoreduction. As a graduate student in the Bocarsly lab at Princeton University, Kailyn currently studies the photo- and electrochemical aspects of CO_2 reduction using manganese complexes.

Rebecca Evans graduated from Rhodes College in 2019 with a B.S. in Chemistry with a minor in Physics and earned her M.A. degree from Princeton University in 2021. She conducted undergraduate research in the field of computational drug design with Dr. Mauricio Cafiero. Rebecca is currently a graduate student in the Bocarsly lab at Princeton University performing density functional theory calculations on various electrochemically active species. Her interests lie in environmental chemistry and theoretical chemical calculations.

Stephanie Dulovic received her B.S. in Biochemistry from Adelphi University in 2020 and her M.A. degree from Princeton University in 2022. Her undergraduate research with Dr. Justyna Widera-Kalinowska was on the topic of photoelectrochemistry, with a focus on inorganic semiconductors and conducting polymers. Stephanie is now a graduate student in the Bocarsly Lab at Princeton University investigating carbon nitride materials and metal alloys as photoelectrocatalysts and electrocatalysts for carbon dioxide reduction.

Andrew B. Bocarsly is a Professor in the Department of Chemistry at Princeton University. He earned his Ph.D. in Chemistry at MIT in 1980 and his B.S. in Chemistry and Physics from UCLA in 1976. His interests lie in transformations of CO_2, photochemistry, semiconductor photoelectrochemistry, and electrocatalysis. He sits on the International Scientific Advisory Board for the International Conference on Carbon Dioxide Utilization (ICCDU) and is an Editorial Advisory Board Member for The Journal of CO_2 Utilization. He cofounded Liquid Light, Inc. in 2009.

ACKNOWLEDGMENTS

The authors thank the many past co-workers from the Bocarsly laboratory, for their central contributions to the research described in this Account. The authors also acknowledge research funding from the National Science Foundation under Grant No. CHE-1308652.

REFERENCES

(1) Agarwal, J.; Shaw, T. W.; Schaefer, H. F., 3rd; Bocarsly, A. B. Design of a Catalytic Active Site for Electrochemical CO_2 Reduction with Mn(I)-Tricarbonyl Species. *Inorg. Chem.* **2015**, *54* (11), 5285−94.

(2) Kuo, H.-Y.; Lee, T. S.; Chu, A. T.; Tignor, S. E.; Scholes, G. D.; Bocarsly, A. B. A cyanide-bridged di-manganese carbonyl complex that photochemically reduces CO_2 to CO. *Dalton Transactions* **2019**, *48* (4), 1226−1236.

(3) Seshadri, G.; Lin, C.; Bocarsly, A. B. A new homogeneous electrocatalyst for the reduction of carbon dioxide to methanol at low overpotential. *J. Electroanal. Chem.* **1994**, *372* (1), 145−150.

(4) Barton, E. E.; Rampulla, D. M.; Bocarsly, A. B. Selective Solar-Driven Reduction of CO_2 to Methanol Using a Catalyzed p-GaP Based Photoelectrochemical Cell. *J. Am. Chem. Soc.* **2008**, *130* (20), 6342−6344.

(5) Blunden, J.; Arndt, D. S. State of the Climate in 2019. *Bulletin of the American Meteorological Society* **2020**, *101* (8), S1−S429.

(6) Hori, Y.; Wakebe, H.; Tsukamoto, T.; Koga, O. Electrocatalytic process of CO selectivity in electrochemical reduction of CO_2 at metal electrodes in aqueous media. *Electrochim. Acta* **1994**, *39* (11), 1833−1839.

(7) Detweiler, Z. M.; White, J. L.; Bernasek, S. L.; Bocarsly, A. B. Anodized Indium Metal Electrodes for Enhanced Carbon Dioxide Reduction in Aqueous Electrolyte. *Langmuir* **2014**, *30* (25), 7593−7600.

(8) Baruch, M. F.; Pander, J. E.; White, J. L.; Bocarsly, A. B. Mechanistic Insights into the Reduction of CO_2 on Tin Electrodes using in Situ ATR-IR Spectroscopy. *ACS Catal.* **2015**, *5* (5), 3148−3156.

(9) Torelli, D. A.; Francis, S. A.; Crompton, J. C.; Javier, A.; Thompson, J. R.; Brunschwig, B. S.; Soriaga, M. P.; Lewis, N. S. Nickel−Gallium-Catalyzed Electrochemical Reduction of CO_2 to Highly Reduced Products at Low Overpotentials. *ACS Catal.* **2016**, *6* (3), 2100−2104.

(10) Paris, A. R.; Chu, A. T.; O'Brien, C. B.; Frick, J. J.; Francis, S. A.; Bocarsly, A. B. Tuning the Products of CO_2 Electroreduction on a Ni_3Ga Catalyst Using Carbon Solid Supports. *J. Electrochem. Soc.* **2018**, *165* (7), H385−H392.
(11) Paris, A. R.; Bocarsly, A. B. Mechanistic insights into C2 and C3 product generation using Ni_3Al and Ni_3Ga electrocatalysts for CO_2 reduction. *Faraday Discuss.* **2019**, *215*, 192−204.
(12) Foster, B.; Paris, A.; Frick, J.; Blasini-Pérez, D.; Cava, R.; Bocarsly, A. Catalytic Mismatching of $CuInSe_2$ and Ni_3Al Demonstrates Selective Photoelectrochemical CO_2 Reduction to Methanol. *ACS Applied Energy Materials* **2020**, *3* (1), 109−113.
(13) Paris, A. R.; Bocarsly, A. B. High-Efficiency Conversion of CO_2 to Oxalate in Water Is Possible Using a Cr-Ga Oxide Electrocatalyst. *ACS Catal.* **2019**, *9* (3), 2324−2333.
(14) Pander, J. E.; Baruch, M. F.; Bocarsly, A. B. Probing the Mechanism of Aqueous CO_2 Reduction on Post-Transition-Metal Electrodes using ATR-IR Spectroelectrochemistry. *ACS Catal.* **2016**, *6* (11), 7824−7833.
(15) Summers, D. P.; Leach, S.; Frese, K. W. The electrochemical reduction of aqueous carbon dioxide to methanol at molybdenum electrodes with low overpotentials. *Journal of Electroanalytical Chemistry and Interfacial Electrochemistry* **1986**, *205* (1), 219−232.
(16) Frese, K. W.; Leach, S. Electrochemical Reduction of Carbon Dioxide to Methane, Methanol, and CO on Ru Electrodes. *J. Electrochem. Soc.* **1985**, *132* (1), 259−260.
(17) Amatore, C.; Saveant, J. M. Mechanism and kinetic characteristics of the electrochemical reduction of carbon dioxide in media of low proton availability. *J. Am. Chem. Soc.* **1981**, *103* (17), 5021−5023.
(18) Schuler, E.; Demetriou, M.; Shiju, N. R.; Gruter, G.-J. M. Towards Sustainable Oxalic Acid from CO_2 and Biomass. *ChemSusChem* **2021**, *14* (18), 3636−3664.
(19) Bocarsly, A. B.; Gibson, Q. D.; Morris, A. J.; L'Esperance, R. P.; Detweiler, Z. M.; Lakkaraju, P. S.; Zeitler, E. L.; Shaw, T. W. Comparative Study of Imidazole and Pyridine Catalyzed Reduction of Carbon Dioxide at Illuminated Iron Pyrite Electrodes. *ACS Catal.* **2012**, *2* (8), 1684−1692.
(20) Yan, Y.; Gu, J.; Bocarsly, A. B. Hydrogen Bonded Pyridine Dimer: A Possible Intermediate in the Electrocatalytic Reduction of Carbon Dioxide to Methanol. *Aerosol and Air Quality Research* **2014**, *14* (2), 515−521.
(21) Halmann, M. Photoelectrochemical reduction of aqueous carbon dioxide on p-type gallium phosphide in liquid junction solar cells. *Nature* **1978**, *275* (5676), 115−116.
(22) Canfield, D.; Frese, K., Jr Reduction of carbon dioxide to methanol on n-and p-GaAs and p-InP. Effect of crystal face, electrolyte and current density. *J. Electrochem. Soc.* **1983**, *130* (8), 1772−1773.
(23) Li, J.; Prentice, G. Electrochemical Synthesis of Methanol from CO_2 in High-Pressure Electrolyte. *J. Electrochem. Soc.* **1997**, *144* (12), 4284.
(24) Watanabe, M.; Shibata, M.; Kato, A.; Azuma, M.; Sakata, T. Design of alloy electrocatalysts for CO_2 reduction: III. The selective and reversible reduction of on Cu alloy electrodes. *J. Electrochem. Soc.* **1991**, *138* (11), 3382.
(25) Ohkawa, K.; Noguchi, Y.; Nakayama, S.; Hashimoto, K.; Fujishima, A. Electrochemical reduction of carbon dioxide on hydrogen-storing materials: Part 3. The effect of the absorption of hydrogen on the palladium electrodes modified with copper. *J. Electroanal. Chem.* **1994**, *367* (1−2), 165−173.
(26) Popić, J. P.; Avramov-Ivić, M.; Vuković, N. Reduction of carbon dioxide on ruthenium oxide and modified ruthenium oxide electrodes in 0.5 M $NaHCO_3$. *J. Electroanal. Chem.* **1997**, *421* (1−2), 105−110.
(27) Bandi, A.; Kühne, H. M. Electrochemical reduction of carbon dioxide in water: analysis of reaction mechanism on ruthenium-titanium-oxide. *J. Electrochem. Soc.* **1992**, *139* (6), 1605.
(28) Qu, J.; Zhang, X.; Wang, Y.; Xie, C. Electrochemical reduction of CO_2 on RuO_2/TiO_2 nanotubes composite modified Pt electrode. *Electrochim. Acta* **2005**, *50* (16−17), 3576−3580.
(29) Barton Cole, E.; Lakkaraju, P. S.; Rampulla, D. M.; Morris, A. J.; Abelev, E.; Bocarsly, A. B. Using a One-Electron Shuttle for the Multielectron Reduction of CO_2 to Methanol: Kinetic, Mechanistic, and Structural Insights. *J. Am. Chem. Soc.* **2010**, *132* (33), 11539−11551.
(30) Morris, A. J.; Mcgibbon, R. T.; Bocarsly, A. B. Electrocatalytic Carbon Dioxide Activation: The Rate-Determining Step of Pyridinium-Catalyzed CO_2 Reduction. *ChemSusChem* **2011**, *4* (2), 191−196.
(31) Yan, Y.; Zeitler, E. L.; Gu, J.; Hu, Y.; Bocarsly, A. B. Electrochemistry of Aqueous Pyridinium: Exploration of a Key Aspect of Electrocatalytic Reduction of CO_2 to Methanol. *J. Am. Chem. Soc.* **2013**, *135* (38), 14020−14023.
(32) Barton Cole, E. E.; Baruch, M. F.; L'Esperance, R. P.; Kelly, M. T.; Lakkaraju, P. S.; Zeitler, E. L.; Bocarsly, A. B. Substituent effects in the pyridinium catalyzed reduction of CO_2 to methanol: further mechanistic insights. *Top. Catal.* **2015**, *58* (1), 15−22.
(33) Liao, K.; Askerka, M.; Zeitler, E. L.; Bocarsly, A. B.; Batista, V. S. Electrochemical reduction of aqueous imidazolium on Pt (111) by proton coupled electron transfer. *Top. Catal.* **2015**, *58* (1), 23−29.
(34) Ertem, M. Z.; Konezny, S. J.; Araujo, C. M.; Batista, V. S. Functional Role of Pyridinium during Aqueous Electrochemical Reduction of CO_2 on Pt(111). *J. Phys. Chem. Lett.* **2013**, *4* (5), 745−748.
(35) Lim, C.-H.; Holder, A. M.; Hynes, J. T.; Musgrave, C. B. Catalytic Reduction of CO_2 by Renewable Organohydrides. *J. Phys. Chem. Lett.* **2015**, *6* (24), 5078−5092.
(36) Lim, C.-H.; Holder, A. M.; Hynes, J. T.; Musgrave, C. B. Reduction of CO_2 to Methanol Catalyzed by a Biomimetic Organo-Hydride Produced from Pyridine. *J. Am. Chem. Soc.* **2014**, *136* (45), 16081−16095.
(37) Alherz, A.; Lim, C.-H.; Hynes, J. T.; Musgrave, C. B. Predicting Hydride Donor Strength via Quantum Chemical Calculations of Hydride Transfer Activation Free Energy. *J. Phys. Chem. B* **2018**, *122* (3), 1278−1288.
(38) Ilic, S.; Alherz, A.; Musgrave, C. B.; Glusac, K. D. Thermodynamic and kinetic hydricities of metal-free hydrides. *Chem. Soc. Rev.* **2018**, *47* (8), 2809−2836.
(39) Keith, J. A.; Carter, E. A. Theoretical Insights into Electrochemical CO_2 Reduction Mechanisms Catalyzed by Surface-Bound Nitrogen Heterocycles. *J. Phys. Chem. Lett.* **2013**, *4* (23), 4058−4063.
(40) Keith, J. A.; Carter, E. A. Electrochemical reactivities of pyridinium in solution: consequences for CO_2 reduction mechanisms. *Chemical Science* **2013**, *4* (4), 1490−1496.
(41) Keith, J. A.; Carter, E. A. Quantum Chemical Benchmarking, Validation, and Prediction of Acidity Constants for Substituted Pyridinium Ions and Pyridinyl Radicals. *J. Chem. Theory Comput.* **2012**, *8* (9), 3187−3206.
(42) Keith, J. A.; Carter, E. A. Theoretical Insights into Pyridinium-Based Photoelectrocatalytic Reduction of CO_2. *J. Am. Chem. Soc.* **2012**, *134* (18), 7580−7583.
(43) Lessio, M.; Carter, E. A. What Is the Role of Pyridinium in Pyridine-Catalyzed CO_2 Reduction on p-GaP Photocathodes? *J. Am. Chem. Soc.* **2015**, *137* (41), 13248−13251.
(44) Lessio, M.; Riplinger, C.; Carter, E. A. Stability of surface protons in pyridine-catalyzed CO_2 reduction at p-GaP photoelectrodes. *Phys. Chem. Chem. Phys.* **2016**, *18* (38), 26434−26443.
(45) Xu, S.; Carter, E. A. 2-Pyridinide as an Active Catalytic Intermediate for CO_2 Reduction on p-GaP Photoelectrodes: Lifetime and Selectivity. *J. Am. Chem. Soc.* **2018**, *140* (28), 8732−8738.
(46) Costentin, C.; Savéant, J.-M.; Tard, C. Catalysis of CO_2 Electrochemical Reduction by Protonated Pyridine and Similar Molecules. Useful Lessons from a Methodological Misadventure. *ACS Energy Letters* **2018**, *3* (3), 695−703.
(47) Keets, K. A.; Cole, E. B.; Morris, A. J.; Sivasankar, N.; Teamey, K.; Lakkaraju, P. S.; Bocarsly, A. B. Analysis of pyridinium catalyzed electrochemical and photoelectrochemical reduction of CO_2:

https://doi.org/10.1021/acs.accounts.1c00643
Acc. Chem. Res. 2022, 55, 944−954

Chemistry and economic impact. *Indian J. Chem.* **2012**, *51A*, 1284−1297.
(48) Hawecker, J.; Lehn, J.-M.; Ziessel, R. Efficient photochemical reduction of CO2to CO by visible light irradiation of systems containing Re(bipy)$(CO)_3$X or Ru(bipy)$_3^{2+}$−Co^{2+}combinations as homogeneous catalysts. *J. Chem. Soc., Chem. Commun.* **1983**, No. 9, 536−538.
(49) Hawecker, J.; Lehn, J.-M.; Ziessel, R. Photochemical and Electrochemical Reduction of Carbon Dioxide to Carbon Monoxide Mediated by (2,2-bipyridine)tricarbonylchlororhenium(I) and Related Complexes as Homogeneous Catalysts. *Helv. Chim. Acta* **1986**, *69* (8), 1990−2012.
(50) Bourrez, M.; Molton, F.; Chardon-Noblat, S.; Deronzier, A. [Mn(bipyridyl)$(CO)_3$Br]: An Abundant Metal Carbonyl Complex as Efficient Electrocatalyst for CO_2 Reduction. *Angew. Chem., Int. Ed.* **2011**, *50* (42), 9903−9906.
(51) Abel, E.; Wilkinson, G. 291. Carbonyl halides of manganese and some related compounds. *Journal of the Chemical Society (Resumed)* **1959**, 1501−1505.
(52) Agarwal, J.; Shaw, T. W.; Stanton, C. J., 3rd; Majetich, G. F.; Bocarsly, A. B.; Schaefer, H. F., 3rd NHC-containing manganese(I) electrocatalysts for the two-electron reduction of CO_2. *Angew. Chem., Int. Ed. Engl.* **2014**, *53* (20), 5152−5.
(53) Agarwal, J.; Stanton, C. J., III; Shaw, T. W.; Vandezande, J. E.; Majetich, G. F.; Bocarsly, A. B.; Schaefer, H. F., III Exploring the effect of axial ligand substitution (X = Br, NCS, CN) on the photodecomposition and electrochemical activity of [MnX(N−C)$(CO)_3$] complexes. *Dalton Transactions* **2015**, *44* (5), 2122−2131.
(54) Smieja, J. M.; Sampson, M. D.; Grice, K. A.; Benson, E. E.; Froehlich, J. D.; Kubiak, C. P. Manganese as a Substitute for Rhenium in CO_2 Reduction Catalysts: The Importance of Acids. *Inorg. Chem.* **2013**, *52* (5), 2484−2491.
(55) Sampson, M. D.; Kubiak, C. P. Manganese Electrocatalysts with Bulky Bipyridine Ligands: Utilizing Lewis Acids To Promote Carbon Dioxide Reduction at Low Overpotentials. *J. Am. Chem. Soc.* **2016**, *138* (4), 1386−1393.
(56) Agarwal, J.; Shaw, T. W.; Schaefer, H. F.; Bocarsly, A. B. Design of a Catalytic Active Site for Electrochemical CO_2 Reduction with Mn(I)-Tricarbonyl Species. *Inorg. Chem.* **2015**, *54* (11), 5285−5294.
(57) Tignor, S. E.; Shaw, T. W.; Bocarsly, A. B. Elucidating the origins of enhanced CO_2 reduction in manganese electrocatalysts bearing pendant hydrogen-bond donors. *Dalton Transactions* **2019**, *48* (33), 12730−12737.
(58) Tignor, S. E.; Kuo, H.-Y.; Lee, T. S.; Scholes, G. D.; Bocarsly, A. B. Manganese-Based Catalysts with Varying Ligand Substituents for the Electrochemical Reduction of CO_2 to CO. *Organometallics* **2019**, *38* (6), 1292−1299.
(59) Kuo, H.-Y.; Tignor, S. E.; Lee, T. S.; Ni, D.; Park, J. E.; Scholes, G. D.; Bocarsly, A. B. Reduction-induced CO dissociation by a [Mn(bpy)$(CO)_4$][SbF_6] complex and its relevance in electrocatalytic CO_2 reduction. *Dalton Transactions* **2020**, *49* (3), 891−900.
(60) Takeda, H.; Koizumi, H.; Okamoto, K.; Ishitani, O. Photocatalytic CO_2 reduction using a Mn complex as a catalyst. *Chem. Commun.* **2014**, *50* (12), 1491−1493.
(61) Torralba-Peñalver, E.; Luo, Y.; Compain, J.-D.; Chardon-Noblat, S.; Fabre, B. Selective Catalytic Electroreduction of CO2 at Silicon Nanowires (SiNWs) Photocathodes Using Non-Noble Metal-Based Manganese Carbonyl Bipyridyl Molecular Catalysts in Solution and Grafted onto SiNWs. *ACS Catal.* **2015**, *5* (10), 6138−6147.
(62) Cheung, P. L.; Machan, C. W.; Malkhasian, A. Y. S.; Agarwal, J.; Kubiak, C. P. Photocatalytic Reduction of Carbon Dioxide to CO and HCO_2H Using fac-Mn(CN)(bpy)$(CO)_3$. *Inorg. Chem.* **2016**, *55* (6), 3192−3198.
(63) Fei, H.; Sampson, M. D.; Lee, Y.; Kubiak, C. P.; Cohen, S. M. Photocatalytic CO_2 Reduction to Formate Using a Mn(I) Molecular Catalyst in a Robust Metal−Organic Framework. *Inorg. Chem.* **2015**, *54* (14), 6821−6828.
(64) Rosser, T. E.; Windle, C. D.; Reisner, E. Electrocatalytic and Solar-Driven CO_2 Reduction to CO with a Molecular Manganese Catalyst Immobilized on Mesoporous TiO_2. *Angew. Chem.* **2016**, *128* (26), 7514−7518.
(65) Zhang, J.-X.; Hu, C.-Y.; Wang, W.; Wang, H.; Bian, Z.-Y. Visible light driven reduction of CO_2 catalyzed by an abundant manganese catalyst with zinc porphyrin photosensitizer. *Applied Catalysis A: General* **2016**, *522*, 145−151.
(66) Lee, T. S. Intermediate States in Solar Light Harvesting: Correlated Triplet Pair Dynamics in Singlet Fission & Photochemical CO_2 Reduction with Manganese Complexes. Ph.D. Thesis, Princeton University, 2019.

https://doi.org/10.1021/acs.accounts.1c00643
Acc. Chem. Res. 2022, 55, 944−954